

# Synthesis and Electronic and Magnetic Characterization of the Ternary Nitride (Fe<sub>0.8</sub>Mo<sub>0.2</sub>)MoN<sub>2</sub>

David S. Bem, Hans P. Olsen, and Hans-Conrad zur Loye\*

Department of Chemistry, Massachusetts Institute of Technology,  
Cambridge, Massachusetts 02139

Received January 31, 1995. Revised Manuscript Received July 13, 1995<sup>⊗</sup>

The new layered ternary transition metal nitride (Fe<sub>0.8</sub>Mo<sub>0.2</sub>)MoN<sub>2</sub> has been synthesized in a single-step reaction by the ammonolysis of the transition-metal oxide, Fe<sub>2</sub>(MoO<sub>4</sub>)<sub>3</sub>. Powder X-ray diffraction data were collected and the structure was refined using the Rietveld method ( $P\bar{3}1c$ ,  $a = 2.8562(1) \text{ \AA}$ ,  $c = 10.9997(4) \text{ \AA}$ ). The structure consists of alternating layers of MN<sub>6</sub> (M = Mo:Fe (1:4)) octahedra and M'N<sub>6</sub> (M' = Mo) trigonal prisms. The magnetic susceptibility data display a maximum at 20 K. Four-probe conductivity measurements indicate poor metallic conductivity with a very small temperature dependence.

## Introduction

Solid state nitrides are of interest because they exhibit technologically useful properties and, consequently, have found utility in such diverse applications as abrasives, electronic materials, and catalysts.<sup>1-5</sup> Despite the potential technological importance of nitrides, only a fairly small number are known and, due to the synthetic challenges of ternary nitride formation, most studies have focused on binary nitrides.<sup>6</sup> We are particularly interested in the syntheses and characterization of ternary nitrides because (1) these materials may have enhanced or improved properties relative to the binaries and (2) relatively few ternary nitrides have been synthesized and fully characterized.<sup>1-3</sup>

In general, nitrides have lower decomposition temperatures than oxides, due to the high bond energy of N<sub>2</sub> (941 kJ/mol) compared to O<sub>2</sub> (499 kJ/mol).<sup>1</sup> Consequently, high-temperature techniques have led to only limited success in the preparation of ternary nitrides and low-to-moderate temperature approaches become essential for preparing both metastable (kinetic) and stable (thermodynamic) compounds. One successful approach has been the use of molecular precursors to make thin films and powders of binary nitrides.<sup>7-9</sup> Nonmolecular precursors,<sup>10</sup> such as high surface area powders,<sup>11</sup> have also been used as an avenue to metastable phases. Ternary nitrides have been synthesized primarily by reacting a transition-metal or main-group

element with an alkali or alkaline earth nitride/amide yielding numerous new phases,<sup>12-23</sup> including Ca<sub>6</sub>-FeN<sub>5</sub>,<sup>15</sup> Li<sub>3</sub>FeN<sub>2</sub>,<sup>24</sup> and NaTaN<sub>2</sub>.<sup>25</sup> Another approach for synthesizing alkali-metal-containing ternary nitrides has been the use of ternary precursors; for example, the ternary nitride LiMoN<sub>2</sub> can be synthesized by the reaction between Li<sub>2</sub>MoO<sub>4</sub> and NH<sub>3</sub>(g).<sup>26</sup>

Although these synthetic methods have been successful, almost all take advantage of the inductive effect, which stabilizes the M-N bond by donation of electrons from an electropositive element.<sup>1,27</sup> This approach limits the number of potential new ternary nitrides to those containing a highly electropositive element such as an alkali or alkaline-earth metal. In the absence of inductive effect stabilization, the formation of binary nitrides rather than ternary nitrides is favored at the high temperatures necessary for reactions (> 1273 K).<sup>3,28</sup> Therefore, to synthesize ternary nitrides in the absence of the inductive effect, new low-temperature synthetic routes need to be developed.

(12) Brokamp, T.; Jacobs, H. *J. Alloys Compd.* **1991**, *176*, 47.

(13) Cordier, G.; Gudat, A.; Kniep, R.; Rabenau, A. *Angew. Chem.* **1989**, *101*, 1689.

(14) Cordier, G.; Gudat, A.; Kniep, R.; Rabenau, A. *Angew. Chem.* **1989**, *101*, 204.

(15) Cordier, G.; Höhn, P.; Kniep, R.; Rabenau, A. *Z. Anorg. Allg. Chem.* **1990**, *591*, 58.

(16) Vennos, D. A.; Badding, M. E.; DiSalvo, F. J. *Inorg. Chem.* **1990**, *29*, 4059.

(17) Vennos, D. A.; DiSalvo, F. J. *J. Solid State Chem.* **1991**, *98*, 318.

(18) Chern, M. Y.; DiSalvo, F. J. *J. Solid State Chem.* **1990**, *88*, 459.

(19) Chern, M. Y.; DiSalvo, F. J. *J. Solid State Chem.* **1990**, *88*, 528.

(20) Chern, M. Y.; Vennos, D. A.; DiSalvo, F. J. *J. Solid State Chem.* **1992**, *96*, 415.

(21) Juza, R.; Langer, K.; Von Benda, K. *Angew. Chem.* **1968**, *80*, 373.

(22) Gudat, A.; Milius, W.; Haag, S.; Kniep, R.; Rabenau, A. *J. Less-Common Met.* **1991**, *168*, 305.

(23) Rauch, P. E.; DiSalvo, F. J. *J. Solid State Chem.* **1992**, *100*, 160.

(24) Gudat, A.; Kniep, R.; Rabenau, A.; Bronger, W.; Ruschewitz, U. *J. Less-Common Met.* **1990**, *161*, 31.

(25) Zachwieja, U.; Jacobs, H. *Eur. J. Solid State Inorg. Chem.* **1991**, *28*, 1055.

(26) Elder, S. H.; Doerr, L. H.; DiSalvo, F. J. *Chem. Mater.* **1992**, *4*, 928.

(27) Etourneau, J.; Portier, J.; Ménil, F. *J. Alloys Compd.* **1992**, *188*, 1.

(28) Marchand, R.; Laurent, Y.; Guyader, J.; L'Haridon, P.; Verdier, P. *J. Eur. Ceram. Soc.* **1991**, *8*, 197.

\* To whom correspondence should be addressed.

⊗ Abstract published in *Advance ACS Abstracts*, August 15, 1995.

(1) DiSalvo, F. J. *Science* **1990**, *247*, 649.

(2) Volpe, L.; Boudart, M. *J. Solid State Chem.* **1985**, *59*, 332.

(3) Toth, L. E. *Transition Metal Carbides and Nitrides*; Academic Press: New York, 1971.

(4) Shakelford, J. F. *Introduction to Materials Science for Engineers*; Macmillan: New York, 1988.

(5) Goldschmidt, H. J. In *Interstitial Alloys*; Plenum Press: New York, 1967; p 214.

(6) Glasson, D. R.; Jayaweera, S. A. A. *J. Appl. Chem.* **1968**, *18*, 65.

(7) LaDuca, R. L.; Wolczanski, P. T. *Inorg. Chem.* **1992**, *31*, 1311.

(8) Winter, C. H.; Sheridan, P. H.; Lewkebandara, T. S.; Heeg, M. J.; Proscia, J. W. *J. Am. Chem. Soc.* **1992**, *114*, 1095.

(9) Holl, M. M. B.; Wolczanski, P. T.; Van Duyne, G. D. *J. Am. Chem. Soc.* **1990**, *112*, 7989.

(10) Ross, C. B.; Wade, T.; Crooks, R. M. *Chem. Mater.* **1991**, *3*, 768.

(11) Chorley, R. W.; Lednor, P. W. *Adv. Mater.* **1991**, *3*, 474.

Our approach, the ammonolysis of ternary oxides,<sup>29–33</sup> has proven to be a successful route for nitride synthesis.<sup>26,28,34</sup> The use of oxide precursors offers the advantage of atomic-level mixing of the metals, which decreases the diffusion distances of the cations and may lower the temperature necessary for reaction. Also, the structure of the precursor may act as a template for product formation<sup>35</sup> and yield phases unattainable by other synthetic routes. We are currently investigating the use of transition metal oxides as precursors to ternary transition-metal nitrides, an approach that has not been extensively explored and that promises to lead to the preparation of new ternary metal nitrides. In this paper we report the synthesis, structure, magnetic, and electronic characterization of  $(\text{Fe}_{0.8}\text{Mo}_{0.2})\text{MoN}_2$ , which was synthesized from the ternary oxide precursor  $\text{Fe}_2(\text{MoO}_4)_3 \cdot 8\text{H}_2\text{O}$ .

### Experimental Section

**$\text{Fe}_2(\text{MoO}_4)_3 \cdot 8\text{H}_2\text{O}$  Synthesis.** Iron(III) molybdate,  $\text{Fe}_2(\text{MoO}_4)_3 \cdot 8\text{H}_2\text{O}$ , was prepared by the method described by Kerr et al.<sup>36</sup> The compound was synthesized by dropwise addition of 50 mL aqueous solution of iron chloride ( $\text{FeCl}_3 \cdot 6\text{H}_2\text{O}$ ; 33.4 mmol; Cerac, 99.99%) to a 500 mL solution of sodium molybdate dihydrate ( $\text{Na}_2\text{MoO}_4 \cdot 2\text{H}_2\text{O}$ ; 50.2 mmol; Aldrich, 99%), which was previously acidified to  $\sim\text{pH}$  4 by the addition of acetic acid. Upon the addition of approximately half of the iron chloride solution, the solution turned deep red and a yellow precipitate was observed. When the addition was complete, the yellow suspension was stirred for 1 h after which the solution was allowed to stand overnight. A yellow solid product was isolated by vacuum filtration and was rinsed with two  $\sim 20$  mL washings of water followed by a single  $\sim 20$  mL washing with anhydrous ethanol. The solid was dried in a vacuum desiccator to constant weight. The product was amorphous by powder X-ray diffraction. The metal ratio of the amorphous powder was determined by ICP (Gailbraith Laboratories Inc.). The ratio  $(\text{Fe weight } \%)_{\text{obs}}/(\text{Mo weight } \%)_{\text{obs}} = 0.39$  agrees with the expected ratio  $(\text{Fe weight } \%)_{\text{theor}}/(\text{Mo weight } \%)_{\text{theor}} = 0.39$ , for  $\text{Fe}_2(\text{MoO}_4)_3$ . Heating the powder to 923 K in a helium atmosphere and measuring the weight change in a Cahn 121 TGA resulted in a weight loss of 29.1%. Assuming that the weight loss of the amorphous yellow powder is entirely due to the loss of water the resulting composition is  $\text{Fe}_2(\text{MoO}_4)_3 \cdot 8.02\text{H}_2\text{O}$ .

**Nitride Synthesis.** The nitride,  $(\text{Fe}_{0.8}\text{Mo}_{0.2})\text{MoN}_2$ , was synthesized by heating  $\sim 0.5$  g of  $\text{Fe}_2(\text{MoO}_4)_3 \cdot 8\text{H}_2\text{O}$  under flowing ammonia at 973 K for 96 h. (**Caution:** Ammonia is a corrosive, toxic gas which must be used in a properly ventilated area.) The oxide precursor,  $\text{Fe}_2(\text{MoO}_4)_3 \cdot 8\text{H}_2\text{O}$ , was placed into an alumina boat, which was then inserted into a quartz flow-through reactor. The sample was heated at 5

K/min to 973 K and soaked for 48 h under flowing ammonia gas (Airco, anhydrous 99.99%; 150  $\text{cm}^3/\text{min}$ ). After 48 h the sample was cooled by turning off the furnace and opening it to the air (cooled from 973 K to 373 K in  $\sim 20$  min). Once the sample had cooled to room temperature, it was removed from the system, ground, and reheated using the identical heating cycle. By trial and error, 973 K was found to be the reaction temperature that gave a pure product. A pure product was obtained only over a narrow temperature range for a given flow rate. After the second heating cycle, the nitride product was stored in a desiccator. Attempts to dissolve the nitride product in acids or bases (HCl,  $\text{HNO}_3$ , aqua regia,  $\text{H}_2\text{SO}_4$ , HF, NaOH) were unsuccessful.

**Characterization.** X-ray Diffraction. Powder X-ray diffraction patterns were collected using a Rigaku RU300  $\theta/\theta$  diffractometer operated at 50 kV and 200 mA with Cu K $\alpha$  radiation. Qualitative phase analysis of the oxide precursor and the reaction product was performed using a continuous scan. NBS silicon was used as an internal standard for lattice parameter determination. Pattern indexing was carried out using the indexing program TREOR.<sup>37</sup> The lattice parameters and theoretical powder patterns were calculated using the NRCVAX crystal structure system.<sup>38</sup> A step-scanned diffraction pattern of  $(\text{Fe}_{0.8}\text{Mo}_{0.2})\text{MoN}_2$  ( $5^\circ \leq 2\theta \leq 120^\circ$ ,  $0.03^\circ$  steps) was used for the Rietveld refinement. Rietveld refinements were performed using the General Structure Analysis System, GSAS.<sup>39</sup>

**Elemental Analysis.** The nitrogen content of the nitride was determined by C, H, N combustion analysis (Oneida) (C 0.02(2) wt %, H 0.00 wt %, N 14.7(2) wt %) and indirectly by thermogravimetric analysis (Cahn 121 TGA). The oxygen impurity was determined by vacuum fusion analysis<sup>40</sup> (LECO, O 1.2 wt %). Due to the insolubility of the nitride product, the metal ratio was determined by energy-dispersive spectroscopy (EDS) on pressed pellets using a JEOL JSM 6400 scanning electron microscope equipped with a Noran Z-max windowless detector (quantification performed using virtual standards on associated Voyager software). The weight ratio of the metals (Mo:Fe) was found to be 73:27. The overall composition based on the metal analysis is  $\text{Fe}_{0.78(2)}\text{Mo}_{1.22(2)}\text{N}_{1.99(2)}\text{O}_{0.14(1)}$ . We were unable to determine whether the oxygen impurity is due to unreacted starting material or surface oxidation.

**Magnetic Measurements.** Magnetic data were collected using a Quantum Design MPMS SQUID magnetometer at temperatures ranging from 5 to 400 K in an applied field of 5 kG. A total of three 6 cm scans were averaged with 32 measurements for each scan length. All data were corrected for the diamagnetic contribution of the Kel-F sample holder.

**Conductivity Measurements.** Temperature-dependent four-probe resistance measurements were performed on pressed pellets using a Keithley 236 source measure unit and a Janis closed-cycle refrigerator (Model ccs-200) by measuring the voltage at a constant current of 75 mA. Pellets were pressed at 5000 psi in air. Attempts to sinter pellets by heating in a nitrogen atmosphere were unsuccessful due to sample decomposition.

### Results and Discussion

The product of the ammonolysis of  $\text{Fe}_2(\text{MoO}_4)_3 \cdot 8\text{H}_2\text{O}$ ,  $\text{Fe}_{0.8}\text{Mo}_{1.2}\text{N}_2$ , is a black crystalline powder which is stable to air and moisture. This nitride was decomposed by heating it in oxygen to 973 K in a TGA (Figure 1), where the products of the oxidation were identified as

(29) Bem, D. S.; Houmes, J. D.; zur Loye, H.-C. In *Soft Chemistry Routes To New Materials*; Trans Tech Publications: Universite de Nantes, 1993; p 183.

(30) Bem, D. S.; Houmes, J. D.; zur Loye, H.-C. In *MRS Symposium Proceeding; Covalent Ceramics II: Non-Oxides*; Barron, A. R., Fischman, G. S., Fury, M. A., Hepp, A. F., Eds.; Boston, MA, 1993; Vol. 327, p 150.

(31) Bem, D. S.; zur Loye, H.-C. *J. Solid State Chem.* **1993**, *104*, 467.

(32) Bem, D. S.; Gibson, C. P.; zur Loye, H.-C. *Chem. Mater.* **1993**, *5*, 397.

(33) Houmes, J. D.; Bem, D. S.; zur Loye, H.-C. In *MRS Symposium Proceeding; Covalent Ceramics II: Non-Oxides*; Barron, A. R., Fischman, G. S., Fury, M. A., Hepp, A. F., Eds.; Boston, MA, 1993; Vol. 327, p 153.

(34) Jagers, C. H.; James, N. M.; Stacy, A. M. *Chem. Mater.* **1990**, *2*, 150.

(35) Banaszak, M. M.; Wolczanski, P. T.; Van Duyne, G. D. *J. Am. Chem. Soc.* **1990**, *112*, 7989.

(36) Kerr, P. F.; Thomas, A. W.; Langer, A. M. *Am. Mineral.* **1963**, *48*, 14.

(37) Werner, P. E.; Eriksson, L.; Westdahl, M. *J. Appl. Crystallogr.* **1985**, *18*, 367.

(38) Larson, A. C.; Lee, F. L.; Le Page, Y.; Webster, M.; Charland, J. P.; Gabe, E. J. In Chemistry Division, NRC, Ottawa, Canada, K1A 0R6.

(39) Larson, A. C.; von Dreele, R. B. In *Lansce, MS-H805: Los Alamos*, 1993.

(40) Harris, W. F. In *Determination of Gaseous Elements in Metals*; Melnick, L. M., Lewis, L. L., Holt, B. D., Eds.; John-Wiley and Sons: New York, 1974; Vol. 40; pp 113.

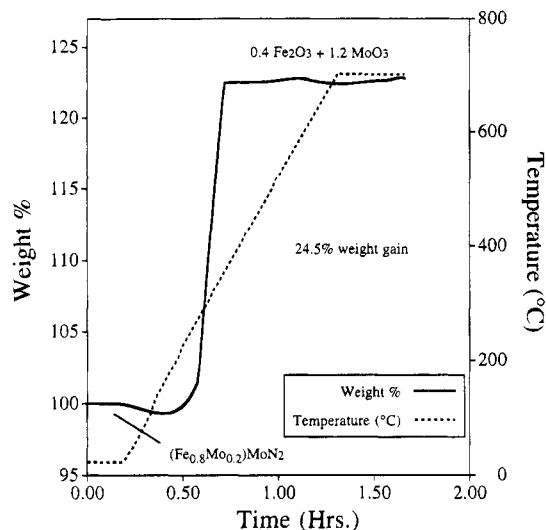


**Figure 1.** Thermogravimetric analysis of  $(\text{Fe}_{0.8}\text{Mo}_{0.2})\text{MoN}_2$  heated to 973 K in flowing  $\text{O}_2$ .

$\text{Fe}_2\text{O}_3$  and  $\text{MoO}_3$  by powder X-ray diffraction. The observed mass gain of 24.52 wt % is smaller than the theoretical mass gain of 26.08 wt % for the oxidation of  $\text{Fe}_{0.8}\text{Mo}_{0.2}\text{N}_2$  to  $0.4 \text{Fe}_2\text{O}_3$  and  $1.2 \text{MoO}_3$ , which indicates that the nitride contains residual oxygen. The mass gain of 24.52 wt % corresponds to a starting composition of  $\text{Fe}_{0.8}\text{Mo}_{0.2}\text{N}_2$  with 1.2 wt % residual oxygen and is consistent with the results from C, H, N combustion analysis.

Indexing of the powder X-ray diffraction data for  $\text{Fe}_{0.8}\text{Mo}_{0.2}\text{N}_2$  gave a hexagonal unit cell of  $a = 2.8562(1) \text{ \AA}$ ,  $c = 10.9997(4) \text{ \AA}$ . There are two possible space groups based on the systematic absences in the indexing:  $P\bar{3}1c$ ,  $P\bar{3}1c$ . A powder pattern was calculated using each space group, and in both cases the calculated intensities closely matched the observed data. Therefore, the higher symmetry space group,  $P\bar{3}1c$ , was chosen and shown to be consistent with the full refinement of the step scanned powder X-ray diffraction data. The metal and nitrogen content of the sample, as determined by elemental analysis, was used as a starting point for the refinement. During the refinement, the individual site occupancies were allowed to vary. Allowing for site mixing of both iron and molybdenum, the structure converged with molybdenum occupying all of the 2(a) site and both iron (0.812(5)) and molybdenum (0.188(5)) occupying the 2(b) site. The refinement converged with  $R_{\text{wp}} = 9.47\%$ ,  $R_{\text{p}} = 7.04\%$ , and  $\chi^2 = 57$ . The data, fit, and residuals are shown in Figure 2, the atomic positions in Table 1, the summary of the refinement parameters in Table 2, and select bond distances in Table 3.

Careful analysis of the X-ray data revealed the presence of a small amount of iron nitride impurity in the sample, which has its 100% peak at  $42.8^\circ 2\theta$  (marked by an "O" in Figure 2). It was not possible to include this additional phase in the Rietveld refinement, as all the other iron nitride peaks have relative intensities of less than 40%. Furthermore, during the refinement we also encountered difficulties with the peak profile descriptions due to irregularly shaped and very broad peaks. All of this is reflected in the high  $\chi^2$  value.

The structure of  $(\text{Fe}_{0.8}\text{Mo}_{0.2})\text{MoN}_2$ , Figure 3, consists of alternating layers of edge-shared octahedra and

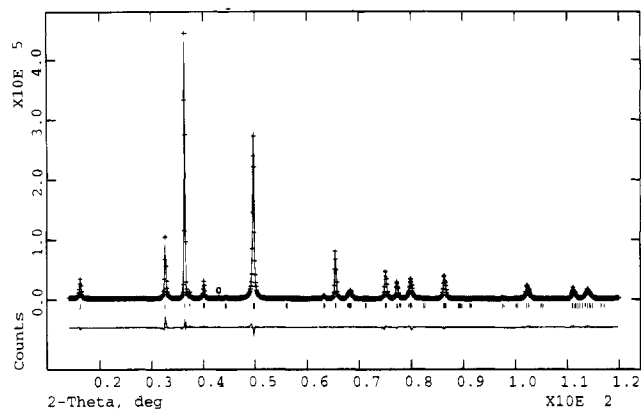


**Figure 2.** Powder X-ray data, including Rietveld fit and residuals, for  $(\text{Fe}_{0.8}\text{Mo}_{0.2})\text{MoN}_2$  (space group  $P\bar{3}1c$ ,  $a = 2.8562(1)$ ,  $c = 10.9997(4) \text{ \AA}$ ,  $R_{\text{wp}} = 9.47\%$ ,  $R_{\text{p}} = 7.04\%$ ). In the upper field the observed data (+) and the calculated fit (black line) are shown. The difference pattern, observed minus calculated, is shown in the lower half, and the short vertical bars indicate the position of possible Bragg reflections. The location of the iron nitride impurity peak is indicated by the marker "O".

**Table 1. Atomic Positions Based on the X-ray Refinements of  $(\text{Fe}_{0.8}\text{Mo}_{0.2})\text{MoN}_2$ , Space Group  $P\bar{3}1c$ ,  $a = 2.8562(1)$ ,  $c = 10.9997(4)$**

metal	Wyckoff	x	y	z	100 $U_{\text{iso}}$	fraction
Mo(1)	2(a)	0	0	1/4	0.69(2)	1.0
Mo(2)	2(b)	0	0	0	1.12(5)	0.188(5)
Fe	2(b)	0	0	0	1.12(5)	0.812(5)
N	4(f)	1/3	2/3	0.1275(5)	1.3(1)	1.0

**Table 2. Crystallographic Data for  $(\text{Fe}_{0.8}\text{Mo}_{0.2})\text{MoN}_2$  from Rietveld Refinement of Powder X-ray Diffraction Data<sup>a</sup>**

powder color	black
formula	$(\text{Fe}_{0.8}\text{Mo}_{0.2})\text{MoN}_2$
formula weight (g/mol)	187.82
space group	$P\bar{3}1c$
a, $\text{ \AA}$	2.8562(1)
c, $\text{ \AA}$	10.9997(4)
V, $\text{ \AA}^3$	77.713(5)
$D_{\text{calc}}$ , g/cm <sup>3</sup>	8.032
$2\theta$ scan range (deg)	5–120
background: cosine Fourier series	6
profile parameters	
$G(w)$	29.96
$L(y)$	22.13
asym <sup>b</sup>	3.13
sample shift <sup>c</sup>	0.0436
ptec <sup>d</sup>	16.25
$R_{\text{wp}}$	9.47
$R_{\text{p}}$	7.04
$\chi^2$	57
$R_{\text{exp}}$	1.25
$\lambda$ , $\text{ \AA}$	1.5405 (Cu K $\alpha$ )

<sup>a</sup> Refinement Rietveld using GSAS with pseudo-Voigt peak shape function. <sup>b</sup> asym = peak asymmetry. <sup>c</sup> Displacement from diffractometer axis:  $S_s = -(\text{shft})(36000)/\pi R$ ;  $R$  (diffractometer radius) = 250 mm, shft (from Rietveld program) =  $9.513 \times 10^{-4}$ . <sup>d</sup> ptec = anisotropic strain broadening.

trigonal prisms, where the octahedra and trigonal prisms are face-shared in the  $c$  direction. The arrangement of the nitrogen and metal atoms can be represented by **AcAcBcBcA**, where **A** and **B** represent the close-packed nitrogen atoms and **c** represents the metal atoms. The trigonal prismatic layer is occupied exclusively by molybdenum, while the octahedral layer contains iron and molybdenum randomly distributed in an approximately 80:20 ratio. The composition, therefore, can be written as  $(\text{Fe}_{0.8}\text{Mo}_{0.2})\text{MoN}_2$ .

**Table 3. Selected Bond Distances for ( $\text{Fe}_{0.8}\text{Mo}_{0.2}\text{MoN}_2$ )**

bond	distance (Å)
Mo(1)-N × 6	2.130(3)
Mo(2)-N <sup>a</sup> × 6	2.164(4)
Fe-Fe <sup>a</sup>	2.8562(1)
Mo-Mo	2.8562(1)
Fe-Mo(1) <sup>a</sup>	2.7499(1)
Fe-Mo(2) <sup>a</sup>	2.8562(1)
Fe-N <sup>a</sup> × 6	2.164(4)
N-N <sup>b</sup>	2.69(1)

<sup>a</sup> Bond distances involving iron are affected by molybdenum occupying 20% of the iron sites. <sup>b</sup> N-N distance between opposing nitrogen sheets within the  $\text{MoN}_2$  layer.

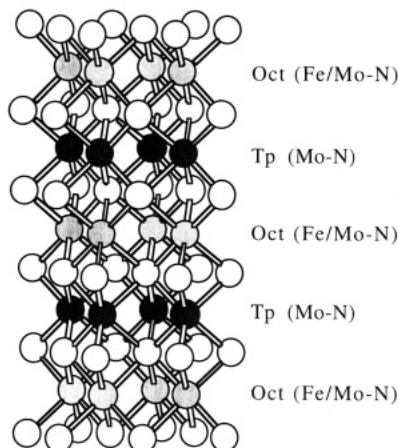


**Figure 3.** Proposed structure for ( $\text{Fe}_{0.8}\text{Mo}_{0.2}\text{MoN}_2$ ). Gray = Fe/Mo, black = Mo, and white = N. The arrangement of the nitrogen and metal atoms can be represented by **AcAcBcBcA**, where **A** and **B** represent the close packed nitrogen atoms, and **c** represents the metal atoms.

( $\text{Fe}_{0.8}\text{Mo}_{0.2}\text{MoN}_2$ ) is isostructural with the known ternary nitride  $\text{FeWN}_2$ <sup>30,41</sup> with Mo occupying all of the tungsten and 20% of the iron sites. Herle et al.<sup>42</sup> reported the structure of  $\text{FeWN}_2$  as being isostructural with that of  $\text{LiMoN}_2$ . While it is possible to index the XRD data to two possible hexagonal unit cells,<sup>31,41</sup> our structural refinement of  $\text{FeWN}_2$ <sup>30,41</sup> indicated that the structure has space group  $P\bar{3}1c$ . Structural refinements using the space group of  $\text{LiMoN}_2$ ,<sup>26</sup>  $R\bar{3}$ , did not converge.

The metal-nitrogen bond distances found in ( $\text{Fe}_{0.8}\text{Mo}_{0.2}\text{MoN}_2$ ) are similar to those found in structurally related nitrides, such as  $\text{FeWN}_2$ ,<sup>41</sup>  $\text{LiMoN}_2$ ,<sup>26</sup> and  $\text{MnMoN}_2$ .<sup>41</sup> The Fe-N bond distance of 2.164(4) Å, although influenced by the presence of some molybdenum on the iron site, is close to that found for the Fe-N bond in  $\text{FeWN}_2$  (2.177(4) Å). The Mo-N bond of 2.130(3) Å, similarly, is comparable to the Mo-N bond lengths of 2.095(4) and 2.091(4) Å found in  $\text{LiMoN}_2$  and of 2.116(2) Å found in  $\text{MnMoN}_2$ . All of the above-mentioned compounds contain layers of edge-shared octahedra alternating with layers of edge-shared trigonal prisms.

Trying to understand the bonding in this class of nitrides is a challenge, and these materials are perhaps described best as being ionic/covalent; consequently, formal oxidation states have to be used with caution. Nonetheless, carrying out a bond valence analysis can be instructive in understanding metal-nitrogen bond lengths and covalency in this class of materials. The

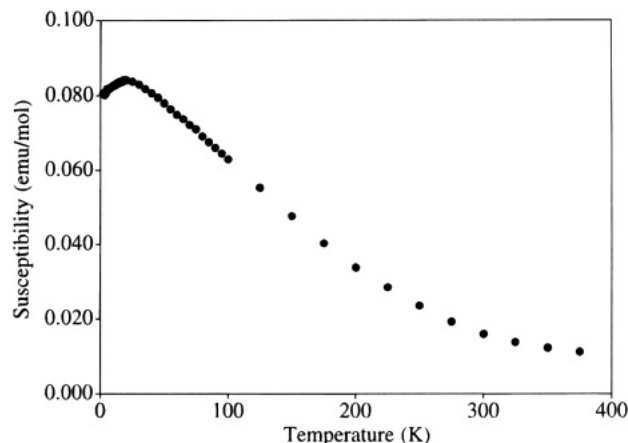


**Figure 4.** Magnetic susceptibility of ( $\text{Fe}_{0.8}\text{Mo}_{0.2}\text{MoN}_2$ ) at 5 kG. The maximum in the susceptibility occurs at 20 K.

application of Brown's bond valence method<sup>43</sup> to nitrides was described by Brese and O'Keefe,<sup>44</sup> who provide bond valence parameters as well as expected bond lengths for regular coordination geometries for some metal-nitride bonds. For example, for iron with valence of 2, coordinated by six nitrogens, the expected bond length is listed as 2.26 Å, which is about 0.1 Å longer than the Fe-N distance in ( $\text{Fe}_{0.8}\text{Mo}_{0.2}\text{MoN}_2$ ) or  $\text{FeWN}_2$ . Using Brown's method, one can calculate a valence for iron of +2.6 in ( $\text{Fe}_{0.8}\text{Mo}_{0.2}\text{MoN}_2$ )—not surprising given the presence of some molybdenum on the iron site.

The trigonal prismatic sites are solely occupied by molybdenum atoms. Using Brown's bond valence method, the valence of the molybdenum is calculated to be +4.8, which indicates that the observed molybdenum-nitrogen bond length is somewhat shorter than that expected for a  $\text{Mo}^{4+}$ -N bond. Both the iron-nitrogen and molybdenum-nitrogen bonds in this material are shorter than expected, which is presumably due to the presence of covalent bonding interactions.

A plot of the magnetic susceptibility as a function of temperature is shown in Figure 4. The susceptibility of ( $\text{Fe}_{0.8}\text{Mo}_{0.2}\text{MoN}_2$ ) exhibits a maximum at 20 K, indicative of antiferromagnetic ordering and similar to what is observed for the isostructural ternary nitride,  $\text{FeWN}_2$ , which has a maximum in the susceptibility at 27 K.<sup>30,45</sup> The ( $\text{Fe}_{0.8}\text{Mo}_{0.2}\text{MoN}_2$ ) sample contains a small amount of iron nitride, a ferromagnetic impurity. Since the precise nitrogen content of iron nitride determines both the Curie temperature and the saturation magnetization it is not possible to accurately correct the magnetic data for the presence of this impurity, which accounts for the otherwise unusually large susceptibility values but does not otherwise influence the magnetic ordering of ( $\text{Fe}_{0.8}\text{Mo}_{0.2}\text{MoN}_2$ ) itself.

Four-probe dc conductivity measurements between 17 and 295 K indicate that the conductivity of ( $\text{Fe}_{0.8}\text{Mo}_{0.2}\text{MoN}_2$ ) exhibits a very small temperature dependence (Figure 5). At 295 K, the observed conductivity is 0.198 S/cm and changes by only 3% (0.198–0.204 S/cm) over the measured temperature range. Similar conductivity data have also been observed in the structurally related ternary nitrides,  $\text{LiMoN}_2$ ,  $\text{MnMoN}_2$ ,  $\alpha$ ,  $\beta$ -

(41) Bem, D. S.; Olsen, H. P.; zur Loye, H.-C. *Inorg. Chem.*, in press.

(42) Herle, P. S.; Yasanthacharya, N. Y.; Hedge, M. S.; Gopalakrishnan, J. *J. Alloys Comp.* **1995**, *217*, 22.

(43) Brown, I. D. *Acta Crystallographica Section B—Structural Science* **1992**, *B48*, 533.

(44) Brese, N. E.; O'Keefe, M. *Struct. Bonding* **1992**, *79*, 309.

(45) Bem, D. S.; zur Loye, H.-C., 1995, unpublished results.

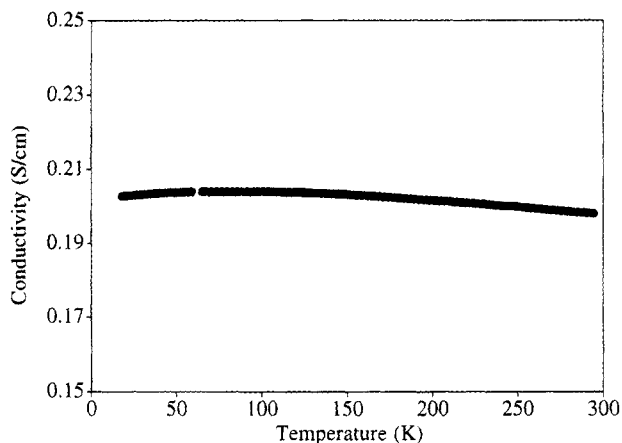


**Figure 5.** Electronic conductivity of  $(\text{Fe}_{0.8}\text{Mo}_{0.2})\text{MoN}_2$  exhibiting temperature independent metallic behavior.

$\text{MnWN}_2$ , and  $\text{FeWN}_2$ .<sup>26,29,31,45,46</sup> The layered structure of  $(\text{Fe}_{0.8}\text{Mo}_{0.2})\text{MoN}_2$  suggests that some anisotropy should be exhibited in the electrical conductivity of the sample. Since the measurement was performed on a pressed pellet the data represent an average of all orientations plus a contribution from grain boundary resistance, which may significantly decrease the conductivity. Therefore, our data should represent a lower limit of the conductivity of  $(\text{Fe}_{0.8}\text{Mo}_{0.2})\text{MoN}_2$ .

(46) zur Loye, H.-C.; Houmes, J. D.; Bem, D. S. In *The Chemistry of Transition Metal Carbides and Nitrides*; Oyama, S. T., Ed.; Blackie Academic and Professional: Glasgow, 1995.

## Summary

The new layered ternary transition metal nitride  $(\text{Fe}_{0.8}\text{Mo}_{0.2})\text{MoN}_2$  has been synthesized in a single-step reaction by the ammonolysis of the transition-metal oxide,  $\text{Fe}_2(\text{MoO}_4)_3 \cdot 8\text{H}_2\text{O}$ . Powder X-ray diffraction data were collected, and the proposed structure was refined using the Rietveld method. The structure consists of alternating layers of  $\text{MN}_6$  ( $M = \text{Mo}:\text{Fe} (1:4)$ ) octahedra and  $\text{M}'\text{N}_6$  ( $M' = \text{Mo}$ ) trigonal prisms. A maximum in the magnetic susceptibility is observed at 20 K. Four probe conductivity measurements indicate that the material has poor metallic conductivity with a very small temperature dependence. The structure and properties of this compound are similar to those found for the isostructural ternary nitride,  $\text{FeWN}_2$ .

**Acknowledgment.** Acknowledgment is made to the donors of The Petroleum Research Fund, administered by the American Chemical Society, for partial support. We would like to thank Joel Houmes for help with the Rietveld refinement. D.S.B. would like to acknowledge 3M and the National Science Foundation for support. We would also like to thank Andrew McInnes for collecting EDS data and Dr. James A Sommers for vacuum fusion analysis.

**Supporting Information Available:** Crystallographic data (18 pages). Ordering information is given on any current masthead page.

CM950050G